Power-Augmentation Control Approach for Arm Exoskeleton Based on Human Muscular Manipulability

Rok Goljat[1,3], Jan Babič[1], Tadej Petrič[1], Luka Peternel[2], Jun Morimoto[3]

Abstract— The paper presents a novel control method for the arm exoskeletons that takes into account the muscular force manipulability of the human arm. In contrast to classical controllers that provide assistance without considering the biomechanical properties of the human arm, we propose a control method that takes into account the configuration of the arm and the direction of the motion to effectively compensate the anisotropic property of the muscular manipulability of the human arm. Consequently, the proposed control method effectively maintains a spherical endpoint manipulability in the entire workspace of the arm. As a result, the proposed method allows the human using the exoskeleton to efficiently perform tasks in arm configurations that are normally unsuitable due to the low manipulability. We evaluated the proposed approach by a preliminary experimental study where a subject wearing a 2 DOF arm-exoskeleton had to move a 4 kg weight between several locations. The results of our study demonstrate that the proposed approach effectively augments the ability of human motor control to perform tasks equally well in the whole arm workspace that include configurations with low intrinsic manipulability.

I. INTRODUCTION

In the past years, robots have been gradually moving from industrial environments into the human daily lives. The main purpose of such robotic systems is to assist humans in various real-life tasks. One of such promising robotic systems are exoskeletons, which are designed to enclose the human body and provide a direct assistance to the motion. The two main applications of exoskeletons are rehabilitation and power augmentation. The former is applicable in medical settings for patients, while the latter is mostly applied in work environments and with physically challenged subjects.

In rehabilitation, the task of the exoskeleton is to move the limbs of impaired humans according to a predefined repetitive motion, which would otherwise be preformed by a physiotherapist. A common approach for exoskeleton control in such case is based on impedance control [1]. Here the robot tries to follow the predefined reference trajectory, while the interaction forces with the user/environment are controlled through a mass-spring-damper system [2]. In this way, stability of the mechanism and safe interaction with the human user can be simplified and maintained.

On the other hand, the task of the exoskeletons in power augmentation is to augment the existing body capabilities of healthy humans or to substitute the impaired abilities of

physically challenged subjects. Here the exoskeleton does not follow a predefined trajectory, but instead amplifies the user's joint torques. The intended joint torque of the user can be obtained either by force/torque measurements [3], [4] or estimated from the muscle activity measurements. The muscle activity can be measured using electromyography (EMG) and mapped to joint torque either by biomechanical models [5], [6], by simple proportional mapping [7], [8] or by adaptive learning [9].

The above-mentioned effort amplification methods amplify the force constantly regardless of the configuration of the user's limb. However, the capability and effectiveness of producing the force at the limb endpoint depends heavily on its current position. A way to evaluate the effectiveness of mechanical systems is by the use of various manipulability measures such as kinematic manipulability, force manipulability and mobility [10], [11], [2]. These measures describe how instantaneous joint displacements are mapped to the end-effector velocities, accelerations or forces. Such endpoint characteristics can be represented as ellipsoids, where the distance from the centre of the ellipsoid to its surface represents the maximal achievable velocity, acceleration or force in the given direction.

A few studies proposed to use manipulability measures in control of robots for human motion augmentation to reduce

Fig. 1. Images of a human wearing an exoskeleton and holding a weight in four different arm configurations.

[1]Dept. for Automation, Biocybernetics and Robotics, Jožef Stefan Institute, Ljubljana, Slovenia, email: rok.goljat@ijs.si

[2]HRI[2] Lab, Dept. of Advanced Robotics, Istituto Italiano di Tecnologia, Genoa, Italy

[3]Dept. of Brain-Robot Interface, ATR Computational Neuroscience Labs, Kyoto, Japan

the human effort in walking [12] and manipulation [13]. However, these methods did not account for specifics of human actuators. In contrast to classical robotic systems, human limbs are actuated by muscles that generate forces which are non-linearly related to the joint torques. To take the properties of human limb actuation into account, several methods have been proposed that estimate the relation between the muscular activation and the resultant motion of the hand [14], [15].

In this paper we propose a control method for the upper-body exoskeletons that takes into account the muscular force manipulability of the human arm. The proposed method accounts for configuration dependent capabilities and effectiveness of the human arm and selectively augments human performance based on the instantaneous arm configuration and the direction of motion. In effect, the approach provides more support in the arm configurations and for the directions of motion where the force manipulability is smaller, and less support for the arm configurations and motion directions with high force manipulability. Consequently, the proposed control method effectively maintains a spherical endpoint manipulability in the entire workspace of the arm. To validate the proposed approach we performed a preliminary experimental study where a subject wearing a 2 DOF arm-exoskeleton had to move a 4 kg weight between several locations and the muscular effort was evaluated using EMG.

II. CONTROL METHOD

The force manipulability measure of a serial manipulator describes the mapping between the joint torques and the forces exerted by the end-effector as a function of the current configuration of the manipulator [10]. Since the human body is not driven by motors in the joints but by muscles, such robotic manipulability measure needs to be updated with the kinematical parameters of the musculoskeletal system of the human arm. Such manipulability measure is called muscular manipulability [14], [15].

We developed an exoskeleton controller that augments human motion based on the muscular manipulability so that the resultant manipulability of the combined human-exoskeleton system maintains a spherical shape throughout the workspace and for any direction of motion. The conceptual model of the proposed approach is shown in Fig. 2.

In the following sub-sections we first describe the classical manipulability measure, then its upgrade to the muscular manipulability measure and finally the musculoskeletal model used to determine the necessary parameters to calculate the muscular manipulability. For the sake of clarity, we describe a planar situation where the manipulability ellipsoid is reduced to an ellipse.

A. Manipulability measure

The manipulability in general describes the effect of a transformation from one coordinate space to another. Mathematically, this describes how a set of all possible values contained within a unit circle transforms to a new set of values. For example in the simple case, where we are
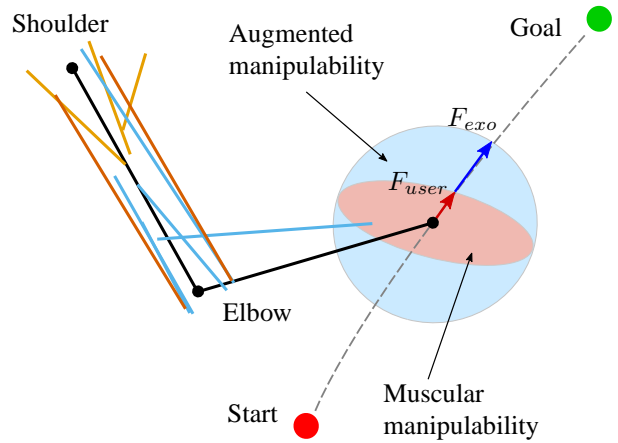
Fig. 2. Conceptual representation of the proposed method. The human arm was modelled as a two segment rigid body mechanism with total of 10 muscles: two biarticular muscles (Biceps short head and Triceps long head), three shoulder muscle (clavicular and sternal part of Deltoid muscle and Pectoralis major) and five elbow muscles (Biceps long head, Triceps lateral and medial head, Brachioradialis and Brachialis). The red ellipse depicts the muscular manipulability of the human arm while the blue circle depicts the resultant manipulability of the combined human-exoskeleton system.

interested in how joint torques transform to end-effector forces, we need to calculate the manipulability from the Jacobian matrix. A set of all values contained within an unit circle is described by

$$||\tau||^2 = \tau^T \tau \leq 1. \tag{1}$$

Since the end effector forces are related to joint torques via the transposed Jacobian matrix of the manipulator, (1) can be rewritten as

$$||\mathbf{J}^T \mathbf{F}||^2 = \mathbf{F}^T (\mathbf{J}\mathbf{J}^T)\mathbf{F} \leq 1. \tag{2}$$

where $\mathbf{J}\mathbf{J}^T$ represents the manipulability ellipse. With singular value decomposition, we can obtain the eigenvectors of this matrix, which correspond to the major and minor axes of the ellipse [10]. The major and minor axes represent the directions in which it is possible to generate higher or lower forces, respectively. This kind of manipulability measure was used in several studies of human motion [15], [16], [17].

B. Muscular manipulability measure

The manipulability measure described in the previous subsection disregards the relation between the forces generated by the muscles and the resultant joint torque. To take this into account we derive the muscular manipulability measure that describes the transformation of the muscle forces to the end-effector forces [14]. First, the transformation from the joint torques to the end-effector forces is described by the Jacobian

$$\tau = \mathbf{J}^T \mathbf{F}. \tag{3}$$

Likewise, the transformation from muscle forces to joint torques can be described by the muscle Jacobian

$$\tau = \mathbf{J}_m^T \mathbf{F}_m, \tag{4}$$

where the muscle Jacobian $\mathbf{J_m}$ is a matrix of muscle moment arms at the joints. The moment arms for extensor muscles
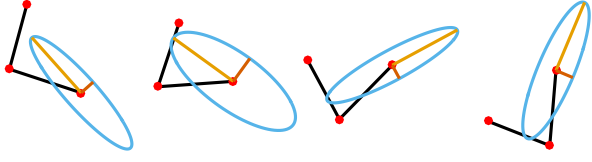
Fig. 3. Four different arm configurations and their corresponding muscular manipulability ellipses.

were defined as the shortest distance between the joint centre and the line connecting the muscle origin and its insertion. The moment arms for extensor muscles were constants selected from the literature [18]. By combining (3) and (4) we get the relation between the muscle forces and the end-effector force as

$$\mathbf{F} = \mathbf{J}^{-T}\mathbf{J}_m^T\mathbf{F}_m. \tag{5}$$

Moreover we use the Hill's model to describe the relation between the muscular activation and the generated force as

$$\mathbf{F} = \mathbf{J}^{-T}\mathbf{J}_m^T\mathbf{F}_h\alpha, \tag{6}$$

where $\mathbf{F_h}$ is the diagonal matrix representing the Hill's muscle force equation and α is the muscular activation level where $||\alpha|| < 1$. This defines the relation

$$\mathbf{F}^T\mathbf{M_m}\mathbf{F} \leq 1, \tag{7}$$

where $\mathbf{M_m}$ represents the muscular manipulability measure defined as

$$(\mathbf{J}^{-T}\mathbf{J}_m\mathbf{F}_h)(\mathbf{J}^{-T}\mathbf{J}_m\mathbf{F}_h)^T. \tag{8}$$

Using the single value decomposition of matrix $\mathbf{M_m}$ we get the major and minor axes of the muscular manipulability ellipse. The major axis represents the direction in which the end-effector has the highest capacity for producing the force, while the minor axis represents the direction in which the capacity for producing force is the lowest. Fig. 3 shows four different arm configurations and their corresponding manipulability ellipses.

The aim of our controller is to augment human motion in such a way that the resultant manipulability of the combined human-exoskeleton system maintains a circular shape throughout the workspace and for any direction of motion. We therefore define the supporting force of the exoskeleton F_{exo} as

$$\mathbf{F}_{exo} = k_{amp}\mathbf{F}_{user}, \tag{9}$$

where k_{amp} represents the amplification factor defined as

$$k_{amp} = \frac{a - ||\mathbf{F}'_{user}||}{a}, \tag{10}$$

with a representing the length of the ellipse major axis and $||\mathbf{F}'_{user}||$ representing the scaled vector of the user's force so that it lies fully within the manipulability ellipse.

Consequently, the exoskeleton provides a variable support based on the direction of the user's force. It offers maximal support when the direction is aligned with the minor axis while it offers no support when the direction is aligned with the major axis of the manipulability ellipse ($k_{amp} = 0$).

C. Musculoskeletal model

To calculate the muscular manipulability measure defined by (8) we modelled the musculoskeletal system of the human arm as a planar two-segment serial mechanism with the first joint representing the shoulder and the second joint the elbow. The wrist was made stiff and was considered to be a part of the forearm. The anthropometric parameters were obtained from [19], [20].

To model the muscles we used the popular Hill-type representation [21] as described by Zajac et al. [22] and defined as

$$F_m = (f_0 f_l f_v \alpha + F_p)cos(\phi) \tag{11}$$

where f_0 represents the optimal muscle force, f_l is the active force-length relationship, f_v is the force-velocity relationship, ϕ is the muscle-tendon penation angle and α is the activation level.

In this model we assumed that the muscles are constantly activated during the motion and hence the passive element has a negligible effect to the generation of force [23]. Since the normalized tendon slack lengths are very small, we also assumed that the tendons are stiff and therefore have a negligible effect on the force generation [22]. Moreover, since all muscles in the human arm have a penation angle lower than 20° [24], we can further simplify the equation (11) and obtain a model of the muscle that can be described as

$$F_m = f_0 f_l f_v \alpha, \tag{12}$$

where $f_0 f_l f_v$ equals to the diagonal matrix of the Hill's muscle force equation denoted as F_h in (8).

Overall, the force generated by the muscle depends on the optimal muscle length, maximal muscle force and tendon slack length. The relations between these parameters and the parameters of (12) are described in detail in [25], [26], [27].

In our model we included a total of ten muscles; two biarticular muscles (Biceps short head and Triceps long head), two shoulder muscle (clavicular and sternal part of Deltoid muscle) and five elbow muscles (Biceps long head, Triceps lateral and medial head, Brachioradialis and Brachialis). To calculate the muscle Jacobian $\mathbf{J_m}$, we determined the muscle origins and insertions from [18]. The musculoskeletal model is shown in Fig. 2.

III. EVALUATION

To evaluate the proposed approach, we performed a preliminary experimental study where a human subject wearing an arm-exoskeleton and holding a 4 kg weight had to perform two motions, one in the region where the muscular manipulability is high and the other where it is low. In the following sub-sections we first describe the experimental protocol, then we introduce the utilized arm-exoskeleton and finally present the results of the evaluation.

A. Experimental protocol

The subject had to perform two movements, each exhibiting different manipulability characteristics throughout the
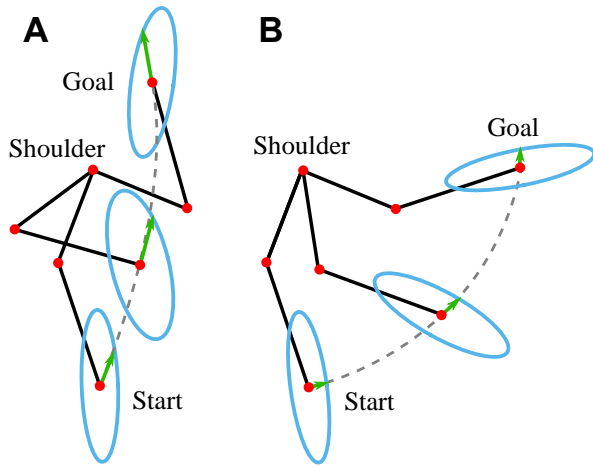
Fig. 4. Arm configurations and the corresponding muscular manipulability ellipses during the two motions performed by the subject. **A:** Motion in the region of high manipulability. **B:** Motion in the region of low manipulability. The arrows represent manipulabilities in the given direction of motion.

path. Fig. 4 shows the arm configurations and the corresponding muscular manipulability ellipses during the two motions performed by the subject. Both motions started at the posture when the subject's arm was freely extended by the body as shown on the left image of Fig. 1. The motion characterized by the high muscular manipulability (left pane of Fig. 4) was performed upwards and as close to the body as possible while the motion characterized by the low muscular manipulability (right pane of Fig. 4) was performed diagonally upwards and outwards towards the fully extended arm configuration as shown on the middle image of Fig. 1. The length of both motions was approximately 70 cm.

The experiment was divided into two sessions of motions. In the first session, the exoskeleton only compensated its own gravity and provided no additional support. In the second session, the exoskeleton provided support through the proposed controller. In each session the subject had 60 s to continuously perform one of the two motions. In the first session the subject was performing the high manipulability motion (left pane of Fig. 4) while in the second session the subject was performing the low manipulability motion (right pane of Fig. 4). The subject was instructed to move the weight by following the rhythm of a metronome, which resulted in approximately 20 cycles of motion.

B. Arm exoskeleton

We implemented our proposed controller on a pneumatically actuated arm exoskeleton (Fig. 1) that was developed at Department of Brain Robot Interface, ATR, Japan [28]. Of the available degrees of freedom, shoulder and elbow joints were used, each actuated by two antagonist pneumatic muscles (PAM). The shoulder joint has approximately 70°range of motion while the elbow joint has approximately 110°. The maximal force of the agonistic muscles was 4000 N while the maximal force of the antagonistic muscles was 600 N.

The implementation of the controller is depicted in Fig. 5. Here, the force generated by the subject (F_{user}) is used to calculate the desired supporting force (F_{exo}) of the
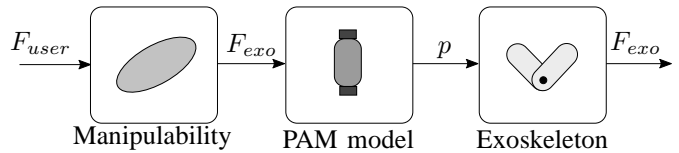
Fig. 5. Implementation of the controller on the pneumatically actuated exoskeleton. The force generated by the subject (F_{user}) is used to calculate the desired supporting force of the exoskeleton (F_{exo}). This force is then used to calculate the desired pressure (p) of the muscles that actuate the exoskeleton.

exoskeleton as defined by (9). Using the dynamic model of the exoskeleton and the pneumatic muscles [29], the corresponding muscle pressure is calculated and applied on the exoskeleton.

C. Results

Average hand trajectories and their standard deviations for the two motions performed by the subject are presented in Fig. 6. Trajectories show little variation between the supported and unsupported motions. The average durations for the motions are shown in Table I.

Fig. 7 shows the support provided by the exoskeleton during the two motions as defined by (10). The starting point of both motions was the same, therefore the support at the beginning of both motions is equal. During the motion characterized by low manipulability, the support was constantly high as shown by the blue trajectory. On the other hand, when the subject was performing the high-manipulability motion, the support provided by the exoskeleton was significantly lower.

To assess the effect of the exoskeleton support on the human effort, we measured and analysed EMG signals of the Biceps long head muscle and Pectoralis minor muscle which are the two dominant arm flexors during the arm-motion in the sagittal plane. The EMG signal was rectified and filtered with a second-order low-pass Butterworth filter with a cut-off frequency of 3 Hz. Fig. 8 shows the normalized sum of EMG activities during the two motions for the unsupported and
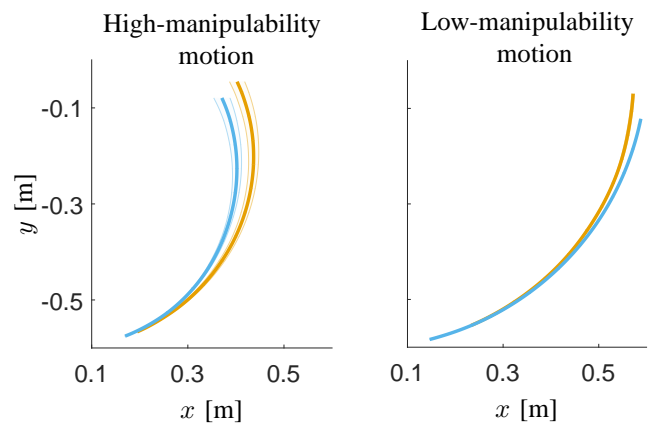
Fig. 6. Average hand trajectories of supported (orange) and unsupported (blue) motions. The left graph shows the trajectories during the high-manipulability motion and the right graph shows the trajectories during the low-manipulability motion.
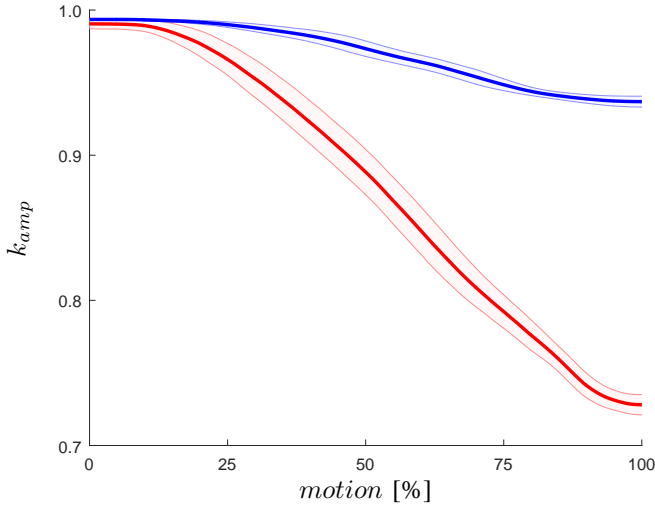
Fig. 7. Support of the exoskeleton during motion. The lines represent the average support of the exoskeleton during high-manipulability motion (red) and low-manipulability motion (blue). Support remains high during low-manipulability motion, while it decreases during high-manipulability motion.
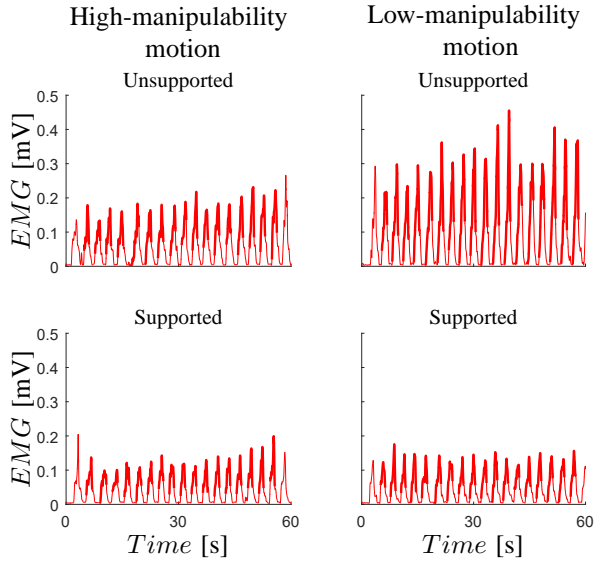
Fig. 8. The graphs represent the normalized sum of EMG activities during the high-manipulability motion (left side graphs) and during the low-manipulability motion (right side graphs). The top graphs correspond to unsupported motions while the bottom graphs correspond to the motions supported by the proposed controller.

supported sessions Thick line sections represent the upward parts of the motions while the thin line sections represent the downward parts. The effect of exoskeleton support is evident for both, high-manipulability and low-manipulability motions. Moreover it is evident that the exoskeleton support was larger during the low-manipulability motion than during the high-manipulability motion. As a consequence, the muscular effort of the subject became equal for both motions.

To quantify the muscular effort we calculated the iEMG by integrating the EMG signals over time. The two bars on the left side of Fig. 9 correspond to iEMG during the high-manipulabilty motion while the two bars on the right side correspond to the low-manipulability motion. Additionally,

the numerical values of iEMG for all combinations of motion and support are given in table I.

IV. CONCLUSION

We proposed a control method for the upper-body exoskeletons that modulates the intrinsic biomechanical property of the human arm. By augmenting the motion of the human based on the instantaneous arm configuration and the direction of motion, the proposed control method effectively maintains a spherical endpoint manipulability in the entire workspace of the human arm.

We validated our approach by a preliminary experimental study where a human subject wearing an arm-exoskeleton and holding a weight had to perform two motions, one in the region where the muscular manipulability is high and the other where it is low. The results show that indeed, the exoskeleton supports more the motion where the manipulability is low than where it is high. In effect, the muscular effort of the subject wearing the exoskeleton became equal for both motions.

In the future, we plan to perform a sensitivity analysis of the musculoskeletal model to determine the level of model simplification that still allow faithful representation of the human arm and the calculation of the muscular manipulability measure. Moreover, we will perform an extensive experimental study where a group of subjects will carry-out
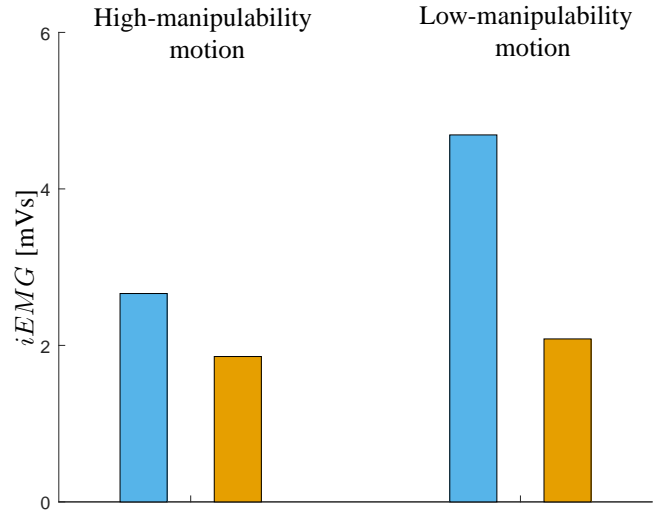
Fig. 9. Integrated EMG for unsupported (blue) and supported motions (orange) . Bars on the left side represent the iEMG during the high-manipulability motion while bars on the right side represent the iEMG during the low-manipulability motion.

TABLE I

MUSCLE EFFORT AND TIME OF MOTION.

Motion (session)	Integrated EMG [mVs]	Motion time [s]
High-manipulability (unsupported)	2.66	1.33
High-manipulability (supported)	1.86	1.32
Low-manipulability (unsupported)	4.69	1.46
Low-manipulability (supported)	2.08	1.32

tasks involving both, the manipulation of objects and interaction with the environment. The aim of this study will be to asses how manipulation of human's intrinsic manipulability by exoskeletons influence human motor control and how such manipulation can enhance human's performance.

ACKNOWLEDGMENTS

REFERENCES

[1] N. G. Tsagarakis and D. G. Caldwell, "Development and control of a soft-actuated exoskeleton for use in physiotherapy and training," *Auton. Robots*, vol. 15, no. 1, pp. 21–33, Jul. 2003.

[2] N. Hogan, "Impedance control: An approach to manipulation: Part ii—implementation," *Journal of dynamic systems, measurement, and control*, vol. 107, no. 1, pp. 8–16, 1985.

[3] J. E. Pratt, B. T. Krupp, C. J. Morse, and S. H. Collins, "The roboknee: an exoskeleton for enhancing strength and endurance during walking," in *Robotics and Automation (ICRA), 2004 IEEE International Conference on*, vol. 3, 2004, pp. 2430–2435 Vol.3.

[4] K. Kong and D. Jeon, "Design and control of an exoskeleton for the elderly and patients," *Mechatronics, IEEE/ASME Transactions on*, vol. 11, no. 4, pp. 428–432, Aug 2006.

[5] J. Rosen, M. Brand, M. B. Fuchs, and M. Arcan, "A myosignal-based powered exoskeleton system," *Systems, Man and Cybernetics, Part A: Systems and Humans, IEEE Transactions on*, vol. 31, no. 3, pp. 210–222, 2001.

[6] C. Fleischer and G. Hommel, "A human–exoskeleton interface utilizing electromyography," *Trans. Rob.*, vol. 24, no. 4, pp. 872–882, Aug. 2008.

[7] D. P. Ferris, K. E. Gordon, G. S. Sawicki, and A. Peethambaran, "An improved powered ankle-foot orthosis using proportional myoelectric control." *Gait & posture*, vol. 23, no. 4, pp. 425–428, Jun. 2006.

[8] T. Lenzi, S. M. M. D. Rossi, N. Vitiello, and M. C. Carrozza, "Intention-based emg control for powered exoskeletons." *IEEE Trans. Biomed. Engineering*, vol. 59, no. 8, pp. 2180–2190, 2012.

[9] L. Peternel, T. Noda, T. Petrič, A. Ude, J. Morimoto, and J. Babič, "Adaptive control of exoskeleton robots for periodic assistive behaviours based on EMG feedback minimisation," *PLoS ONE*, vol. 11, no. 2, p. e0148942, Feb 2016.

[10] T. Yoshikawa, "Manipulability of Robotic Mechanisms," *The International Journal of Robotics Research*, vol. 4, no. 2, pp. 3–9, jun 1985.

[11] ——, "Dynamic manipulability of robot manipulators," in *Robotics and Automation. Proceedings. 1985 IEEE International Conference on*, vol. 2. IEEE, 1985, pp. 1033–1038.

[12] W. Kim, S. Lee, M. Kang, J. Han, and C. Han, "Energy-efficient gait pattern generation of the powered robotic exoskeleton using dme," in *2010 IEEE/RSJ International Conference on Intelligent Robots and Systems*, Oct 2010, pp. 2475–2480.

[13] T. Petrič, R. Goljat, and J. Babič, "Augmentation of human arm motor control by isotropic force manipulability," in *2016 IEEE/RSJ International Conference on Intelligent Robots and Systems (IROS)*, Oct 2016, pp. 696–701.

[14] K. Ohta, Y. Tanaka, I. Kawate, and T. Tsuji, "Human muscular mobility ellipsoid: End-point acceleration manipulability measure in fast motion of human upper arm," *Journal of Biomechanical Science and Engineering*, vol. 9, no. 3, pp. 14–00 207, 2014.

[15] Y. Tanaka, N. Yamada, K. Nishikawa, I. Masamori, and T. Tsuji, "Manipulability analysis of human arm movements during the operation of a variable-impedance controlled robot," in *2005 IEEE/RSJ International Conference on Intelligent Robots and Systems*. IEEE, 2005, pp. 1893–1898.

[16] K. Hara, R. Yokogawa, and A. Yokogawa, "A graphical method for evaluating static characteristics of the human finger by force manipulability," in *Robotics and Automation, 1998. Proceedings. 1998 IEEE International Conference on*, vol. 2. IEEE, 1998, pp. 1623–1628.

[17] P. N. Sabes, M. I. Jordan, and D. M. Wolpert, "The role of inertial sensitivity in motor planning," *The Journal of neuroscience*, vol. 18, no. 15, pp. 5948–5957, 1998.

[18] J. Wood, S. Meek, and S. Jacobsen, "Quantitation of human shoulder anatomy for prosthetic arm control—ii. anatomy matrices," *Journal of biomechanics*, vol. 22, no. 4, pp. 309–325, 1989.

[19] K. R. Holzbaur, W. M. Murray, and S. L. Delp, "A model of the upper extremity for simulating musculoskeletal surgery and analyzing neuromuscular control," *Annals of biomedical engineering*, vol. 33, no. 6, pp. 829–840, 2005.

[20] J. Langenderfer, S. A. Jerabek, V. B. Thangamani, J. E. Kuhn, and R. E. Hughes, "Musculoskeletal parameters of muscles crossing the shoulder and elbow and the effect of sarcomere length sample size on estimation of optimal muscle length," *Clinical Biomechanics*, vol. 19, no. 7, pp. 664–670, 2004.

[21] A. Hill, "The heat of shortening and the dynamic constants of muscle," *Proceedings of the Royal Society of London B: Biological Sciences*, vol. 126, no. 843, pp. 136–195, 1938.

[22] F. E. Zajac, "Muscle and tendon properties models scaling and application to biomechanics and motor," *Critical reviews in biomedical engineering*, vol. 17, no. 4, pp. 359–411, 1989.

[23] S. Jo, "A computational neuromusculoskeletal model of human arm movements," *International Journal of Control, Automation and Systems*, vol. 9, no. 5, pp. 913–923, 2011.

[24] M. A. Lemay and P. E. Crago, "A dynamic model for simulating movements of the elbow, forearm, and wrist," *Journal of biomechanics*, vol. 29, no. 10, pp. 1319–1330, 1996.

[25] F. M. Colacino, R. Emiliano, and B. R. Mace, "Subject-specific musculoskeletal parameters of wrist flexors and extensors estimated by an emg-driven musculoskeletal model," *Medical engineering & physics*, vol. 34, no. 5, pp. 531–540, 2012.

[26] T. S. Buchanan, D. G. Lloyd, K. Manal, and T. F. Besier, "Neuromusculoskeletal modeling: estimation of muscle forces and joint moments and movements from measurements of neural command," *Journal of applied biomechanics*, vol. 20, no. 4, p. 367, 2004.

[27] N. Lan, "Stability analysis for postural control in a two-joint limb system," *IEEE Transactions on neural systems and rehabilitation engineering*, vol. 10, no. 4, pp. 249–259, 2002.

[28] T. Noda, T. Teramae, B. Ugurlu, and J. Morimoto, "Development of an upper limb exoskeleton powered via pneumatic electric hybrid actuators with bowden cable," in *2014 IEEE/RSJ International Conference on Intelligent Robots and Systems*. IEEE, 2014, pp. 3573–3578.

[29] L. Peternel, B. Ugurlu, J. Babič, and J. Morimoto, "Assessments on the improved modelling for pneumatic artificial muscle actuators," in *Advanced Robotics (ICAR), 2015 International Conference on*. IEEE, 2015, pp. 34–39.